Nonisolated High Step-Up DC–DC Converters Adopting Switched-Capacitor Cell

Gang Wu, *Student Member, IEEE*, Xinbo Ruan, *Senior Member, IEEE*, and Zhihong Ye, *Member, IEEE*

***Abstract*—In a photovoltaic (PV)- or fuel-cell-based grid-connected power system, a high step-up dc–dc converter is required to boost the low voltage of a PV or fuel cell to a relatively high bus voltage for the downstream dc–ac grid-connected inverter. To integrate the advantages of the high voltage gain of a switched-capacitor (SC) converter and excellent output regulation of a switching-mode dc–dc converter, a method of combining the two types of converters is proposed in this paper. The basic idea is that when the switch is turned on, the inductor is charged, and the capacitors are connected in series to supply the load, and when the switch is turned off, the inductor releases energy to charge multiple capacitors in parallel, whose voltages are controlled by a pulsewidth modulation technique. Thus, a high voltage gain of the dc–dc converter can be obtained with good regulation. Based on this principle, a series of new topologies are derived, and the operating principles and voltage gains of the proposed converters are analyzed. Finally, the design of the proposed converter is given, and the experiment results are provided to verify the theoretical analysis.**

***Index Terms*—High efficiency, high voltage gain, nonisolated, switched capacitor (SC).**

I. Introduction

THE mass usage of traditional fossil energy has adversely affected the environment on a global scale, such as environmental pollution and greenhouse effect. Meanwhile, there has been a growing demand for energy with the development of society. Since traditional fossil energy is not renewable, it is faced with the problem of energy shortage. Therefore, it is necessary to develop new energy that is clean and renewable to replace traditional fossil energy. Solar energy and hydrogen energy are promising, and photovoltaic (PV) and fuel cell power generation as the utilization method of the two new energy types have been applied on a large scale [1]–[6].

In a single-phase system with a two-stage structure, if the line voltage is 220 V, the bus voltage of the grid-connected inverter needs to be as high as 380 V. However, the output voltages of PV and fuel cells are generally ranged from 25 to 45 V, which are much lower than the bus voltage. Thus, a dc–dc converter with a high voltage gain is needed to boost the outputs of PV and fuel cells. By increasing the turns ratio of the transformer in isolated converters, a high voltage gain can be obtained. However, a too large turns ratio will lead to a large leakage inductor. As a result, the voltage stress of the switch will be increased, whereas the efficiency of the converter is degraded [7]–[9].

Among the nonisolated dc–dc converters, the boost converter is usually used for voltage step-up. However, the duty cycle will approach to unity when the output voltage is much higher than the input voltage. Thus, the current ripple of the inductor and turn-off current of the power device are large, which results in large conduction loss, switching loss, and thus low efficiency [10], [11]. By cascading another boost converter, a high voltage gain can be easily obtained [12]. However, too many components are required, leading to high cost and low overall efficiency.

Introducing a coupled inductor into the nonisolated converter and selecting an appropriate turns ratio of the coupled inductor can increase the voltage gain effectively. However, a snubber circuit is needed to absorb the energy stored in the leakage inductor. This will lead to circuit complexity and low efficiency. In [13]–[17], the active-clamp technique is incorporated to suppress the voltage spike of the switch and regenerate the energy stored in the leakage inductor to the load, which leads to improved efficiency. However, the input current of the proposed converter is pulsating, and the resonance between the leakage inductor and the parasitic capacitor of the output diode is severe.

The switched-capacitor (SC) converter can obtain a high voltage gain, but the input current is pulsating, and the load and line regulation is poor. Meanwhile, the voltage gain is predetermined by the circuit structure [18]. By incorporating the SC structure into the switching-mode dc–dc converters, the voltage gain can be dramatically increased with an appropriate duty cycle while the voltage regulation is achieved [18]–[20]. Moreover, the pulsating input current can be reduced. However, there still exist some deficiencies in the converters. For example, the circuit proposed in [18] cannot be infinitely extended. Thus, in the situation where an enormous voltage gain is needed, the duty cycle is still relatively large. Moreover, the voltage gain of the elementary circuit proposed in [19] and [20] is not high enough. When an extension circuit is added to increase the voltage gain further, the topology will be complicated and with high cost.

The voltage gain of the SC converter is high, but the output voltage is not regulated. The output regulation of the nonisolated switching-mode dc–dc converter is excellent, but the

Manuscript received December 2, 2013; revised March 18, 2014; accepted April 23, 2014. Date of publication May 29, 2014; date of current version December 19, 2014. This work was supported by Lite-On Technology Corporation.

G. Wu and X. Ruan are with the Aero-Power Sci-Tech Center, College of Automation Engineering, Nanjing University of Aeronautics and Astronautics, Nanjing 210016, China (e-mail: wugang@nuaa.edu.cn; ruanxb@nuaa.edu.cn).

Z. Ye is with the Power SBG ATD-NJ R&D Center, Lite-On Technology Corporation, Nanjing 210019, China (e-mail: Sam.Ye@liteon.com).

Color versions of one or more of the figures in this paper are available online at http://ieeexplore.ieee.org.

Digital Object Identifier 10.1109/TIE.2014.2327000

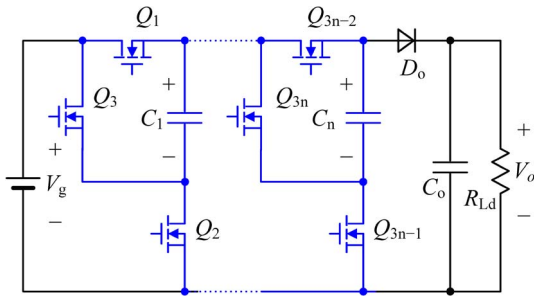

Fig. 1. Step-up SC converter.

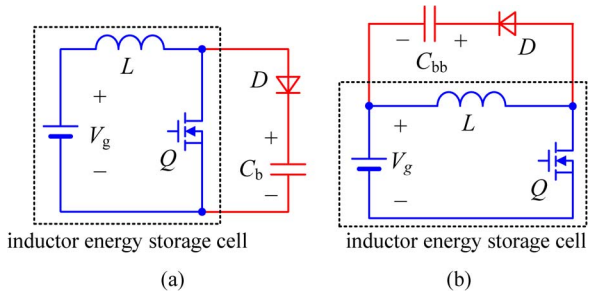

Fig. 2. SC structure with a single inductor energy storage cell. (a) Boost. (b) Buck–boost.

voltage gain cannot be too high for achieving high efficiency. This paper proposes a combination method of the SC converter and the switching-mode dc–dc converter. The basic approach is introducing multiple capacitors into the switching-mode dc–dc converters. When the switch is off, the energy released from the inductor is used to charge the capacitors in parallel. When the switch is on, the capacitors are connected in series to supply the load. Thus, the voltage gain is increased, and the duty cycle is decreased, leading to small ripple current and turn-off current of the switch, and high efficiency can be expected. Meanwhile, the voltages of the capacitors are well regulated, thus achieving a tightly regulated output voltage. In addition, the new converters proposed in this paper can be infinitely extended when an enormous voltage gain is needed.

II. Basic SC Configurations Adopting Inductor Energy Storage Cell

Fig. 1 shows the topology of a step-up SC converter. When switches $Q_1, Q_2, Q_4, Q_5, \ldots, Q_{3n-2}, Q_{3n-1}$ conduct, and $Q_3, Q_6, \ldots, Q_{3n}$ are turned off, the input voltage source charges the SCs $C_1, C_2, \ldots, C_n$ in parallel. When $Q_1, Q_2, Q_4, Q_5, \ldots, Q_{3n-2}, Q_{3n-1}$ are turned off, and $Q_3, Q_6, \ldots, Q_{3n}$ conduct, $C_1, C_2, \ldots, C_n$ and the voltage source are connected in series to supply the load. Therefore, the output voltage is $(n+1) \cdot V_g$, where n is the number of the SCs, and V_g is the input voltage. It can be seen that it is effective to increase the voltage gain by charging the SCs in parallel and discharging in series. However, the output voltage of this step-up SC converter cannot be regulated, and it varies with the input voltage.

To solve the problem, Fig. 2 shows an inductor energy storage cell that is used to charge the SCs. When switch Q is on, the input voltage source charges the inductor. When Q is off, the inductor charges the SC. The voltage of the SC can be regulated by adjusting the duty cycle of the switch.

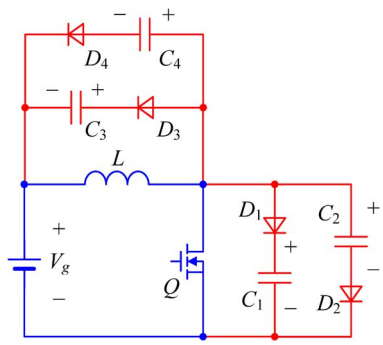

Fig. 3. SC structure sharing an inductor energy storage cell.

The circuit shown in Fig. 2(a) is similar to a boost converter, whereas the circuit shown in Fig. 2(b) resembles a buck–boost converter. Hereinafter, the SC is called the boost capacitor when it is in parallel with the switch, and the SC is called the buck–boost capacitor when it is in parallel with the inductor. Diode D is used to prevent capacitor C from being shorted [see Fig. 2(a)] or being in parallel with the input voltage source [see Fig. 2(b)] when Q is on. Obviously, the positions of the diode and the SC can be exchanged.

At steady state, the volt–second relationship of the inductor is given as

$$V_g D_y T_s = (V_{Cb} - V_g)(1 - D_y)T_s = V_{Cbb}(1 - D_y)T_s \quad (1)$$

where V_{Cb} and V_{Cbb} are the voltages of the boost capacitor and the buck–boost capacitor, respectively, and D_y is the duty cycle. Then, V_{Cb} and V_{Cbb} can be derived as

$$V_{Cb} = \frac{V_g}{1 - D_y} \quad (2)$$

$$V_{Cbb} = \frac{D_y V_g}{1 - D_y}. \quad (3)$$

Obviously, the voltage of the boost capacitor is higher than that of the buck–boost capacitor with the same duty cycle.

When the two SC structures shown in Fig. 2 share the inductor energy storage cell and two position arrangements of the diode and capacitor, the SC structure sharing an inductor energy storage cell can be derived as shown in Fig. 3. When switch Q is on, the input source charges the inductor. While switch Q is off, C_1, C_2, C_3, and C_4 are simultaneously charged by the inductor.

III. Nonisolated High Step-Up DC–DC Converter With Single-Inductor-Energy-Storage-Cell-Based SCs (SIESC-SCs)

A. Derivation of High Step-Up Converter With SIESC-SCs

To obtain a high voltage gain, the SCs in Fig. 3 should be connected in series as many as possible when switch Q is on. Moreover, the polarities of the capacitors to be connected in series should be different at the connection point. Since the positive terminals of C_2 and C_4 are directly connected, C_2 and C_4 cannot be connected in series. Likewise, C_1 and C_3 cannot be connected in series because the negative terminals of the two capacitors are connected through the input voltage source.

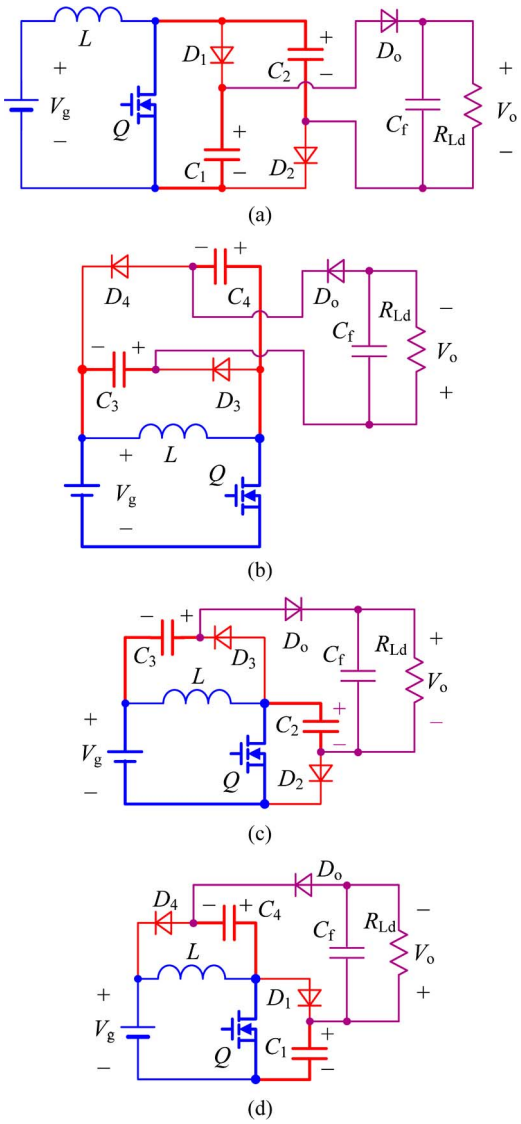

Fig. 4. High step-up converters with SIESC-SCs derived from (a) boost converter, (b) buck–boost converter, (c) Type-I boost/buck–boost-based converter, and (d) Type-II boost/buck–boost-based converter.

Therefore, only two of the four SCs can be connected in series in Fig. 3. The possible connection methods of two SCs in series are shown in Fig. 4, where the two SCs that can be connected in series are shown with thick lines. C_1 and C_2 are connected in series through switch Q as shown in Fig. 4(a), C_3 and C_4 are connected in series through Q as shown in Fig. 4(b), C_2 and C_3 are connected in series through Q as shown in Fig. 4(c), and C_1 and C_4 are connected in series through Q as shown in Fig. 4(d).

The series-connected capacitors are connected to the output filter capacitor C_f and load resistor R_{Ld} through diode D_o. Noted that D_o is used to prevent the output from being in parallel with one of the SCs when the power switch Q is turned off and the diodes conduct. The converters shown in Fig. 4(a) and (b) have been presented in [17].

B. Operating Principle

Referring to Fig. 4(a), when the inductor current is continuous, there exist two operating modes for a high step-up converter with SIESC-SCs derived from the boost converter. The topological equivalent circuits are shown in Fig. 5. When Q is conducting, as shown in Fig. 5(a), the input voltage source charges the inductor. Meanwhile, C_2 is in series with C_1 to supply the load through Q. When Q is turned off, as shown in Fig. 5(b), the inductor charges C_1 and C_2 in parallel, and the load is powered by C_f. Since the two SCs in series when Q is conducting are both the boost capacitors, the voltage gain is

$$M = \frac{V_o}{V_g} = \frac{1}{1-D_y} + \frac{1}{1-D_y} = \frac{2}{1-D_y}. \tag{4}$$

Similarly, the topological equivalent circuits for the other three converters in Fig. 4 are shown in Figs. 6–8, respectively. In Fig. 6, when switch Q is turned on, the input voltage

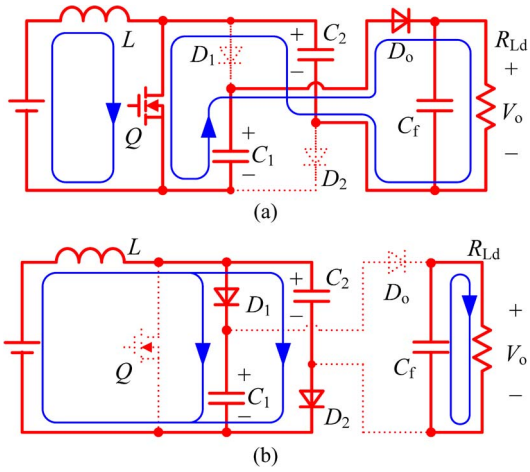

Fig. 5. Operating modes of a high step-up converter with SIESC-SCs derived from boost. (a) Q is on. (b) Q is off.

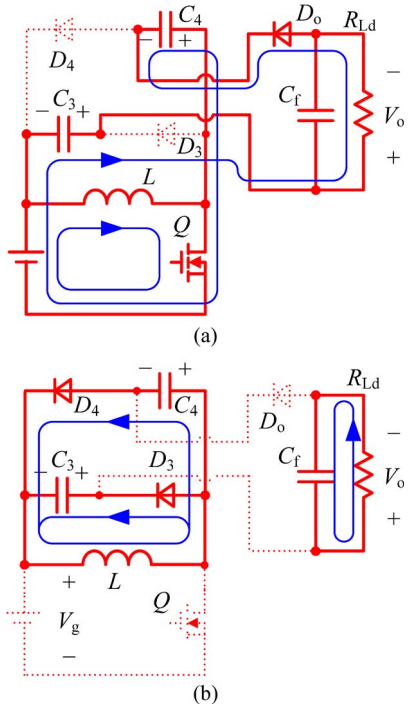

Fig. 6. Operating modes of a high step-up converter with SIESC-SCs derived from buck–boost. (a) Q is on. (b) Q is off.

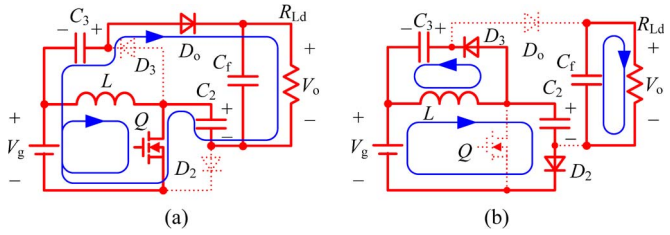

Fig. 7. Operating modes of a high step-up converter with SIESC-SCs derived from Type-I boost/buck–boost-based converter. (a) Q is on. (b) Q is off.

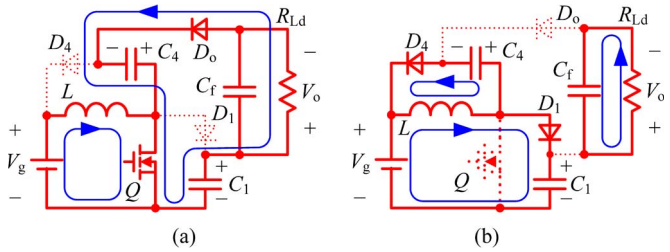

Fig. 8. Operating modes of a high step-up converter with SIESC-SCs derived from Type-II boost/buck–boost-based converter. (a) Q is on. (b) Q is off.

source charges the inductor. Meanwhile, C_4 is in series with the voltage source and C_3 to supply the load through Q. When Q is turned off, the inductor charges C_3 and C_4 in parallel, and the load is powered by C_f. In this converter, both the SCs are the buck–boost capacitors, and the two capacitors are in series with the voltage source to supply the load. Thus, the voltage gain of a high step-up converter with SIESC-SCs derived from buck–boost converter is

$$M = \frac{V_o}{V_g} = \frac{D_y}{1-D_y} + \frac{D_y}{1-D_y} + 1 = \frac{1+D_y}{1-D_y}. \quad (5)$$

In Fig. 7, when Q is turned on, the input voltage source charges the inductor. Meanwhile, C_2 is in series with the voltage source and C_3 to supply the load through Q. When Q is turned off, the inductor charges C_2 and C_3 simultaneously, and the load is powered by C_f. In this converter, one of the SCs is the boost capacitor, and the other one is the buck–boost capacitor. The two capacitors and the voltage source are connected in series to supply the load. Thus, the voltage gain of a high step-up converter with SIESC-SCs derived from Type-I boost/buck–boost-based converter is

$$M = \frac{V_o}{V_g} = \frac{1}{1-D_y} + \frac{D_y}{1-D_y} + 1 = \frac{2}{1-D_y}. \quad (6)$$

In Fig. 8, when Q is turned on, the input voltage source charges the inductor. Meanwhile, C_4 is in series with C_1 to supply the load through Q. When Q is off, the inductor charges C_1 and C_4 simultaneously, and the load is powered by C_f. In this converter, one of the SCs is the boost capacitor, and the other one is the buck–boost capacitor. Therefore, the voltage gain of a high step-up converter with SIESC-SCs derived from Type-II boost/buck–boost-based converter is

$$M = \frac{V_o}{V_g} = \frac{1}{1-D_y} + \frac{D_y}{1-D_y} = \frac{1+D_y}{1-D_y}. \quad (7)$$

C. Comparison of the Four Converters With SIESC-SCs

The features and voltage gains of the converters in Fig. 4 are listed in Table I, where $M = V_o/V_g$. Obviously, the voltage gains of the proposed converters are higher than that of the switching-mode dc–dc converters with the same duty cycle. The two SCs in Fig. 4(a) are both boost capacitors, and the voltage gain of this converter is relatively high. Although one SC is a boost capacitor and the other one is a buck–boost capacitor in Fig. 4(c), the voltage gain of the converter is still as high as that of the converter in Fig. 4(a) because of the inclusion of the input voltage source. The voltage gains of the converters shown in Fig. 4(a) and (c) are higher than that of the converters shown in Fig. 4(b) and (d). In the converter shown in Fig. 4(a), the input voltage source cannot power the load directly. The energy from the input voltage source is first stored in the SCs and then released to the load by the SCs. In the converter shown in Fig. 4(c), part of the energy is directly transferred to the load from the input source when the switch conducts. Therefore, it can be expected that the efficiency of the converter in Fig. 4(c) is higher than that in Fig. 4(a). Unfortunately, the input current of the converter shown in Fig. 4(c) is pulsating.

IV. Nonisolated High Step-Up DC–DC Converter With Multiple-Inductor-Energy-Storage-Cell-Based SCs (MIESC-SCs)

A. Derivation of High Step-Up Converter With MIESC-SCs

If the voltage gain needs to be increased further, based on the converters in Fig. 4, more SCs can be added to be in series with existing SCs. Taking the converter shown in Fig. 4(c) as an example, the SC C_3 is added as shown in Fig. 9(a), and one more inductor energy storage cell consisting of V_{g2}, Q_2, and L_2 is added to replenish energy for C_3. When Q_1 and Q_2 simultaneously conduct, V_{g1} charges L_1 through Q_1, and V_{g2} charges L_2 through Q_2. C_1, C_2, C_3, and the input voltage source V_{g1} are in series to supply the load, as shown by thick lines in Fig. 9(a). When Q_1 and Q_2 are turned off simultaneously, L_1 charges C_1 and C_2 via D_1 and D_2, respectively, and L_2 charges C_3 via D_3.

As Q_1 and Q_2 are turned on and off synchronously, Q_1 and Q_2 are expected to share one switch for simplification. Thus, the voltage source V_{g2} is separated into two sources V_{g2a} and V_{g2b}, as shown in Fig. 9(b). By connecting points A and B, the branch consisting of C_2 and Q_1 is in parallel with the branch consisting of V_{g2a} and Q_2. Thus, V_{g2a} can be substituted by C_2, and Q_2 can be replaced by Q_1, and the branch consisting of V_{g2a} and Q_2 can be removed. Then, a high step-up converter with double-inductor-energy-storage-cell-based SCs derived from Type-I boost/buck–boost-based converter is obtained as shown in Fig. 10, where the voltage source V_{g2b} is formed with C_b. When Q is on, C_2 and C_b are connected in series to charge L_2, and C_1, C_2, C_3, and V_g are in series to power the load. When Q is turned off, the current of L_1 charges C_1 and C_2, whereas the current of L_2 charges C_3. As D_2 and D_3 conduct at the same time, the voltages of C_b and C_3 are equal. Similarly, a high step-up converter with MIESC-SCs derived from Type-I boost/buck–boost-based converter is obtained as shown in Fig. 11 by adding multiple SCs.

TABLE I
COMPARISON OF HIGH STEP-UP CONVERTERS WITH SIESC-SCS

High step-up converters with SIESC-SCs	Number of boost capacitors	Number of buck-boost capacitors	The input source is in series with the capacitors?	Voltage gain
Converter in Fig. 4(a)	2	0	NO	$M=\frac{2}{1-D_y}$
Converter in Fig. 4(b)	0	2	YES	$M=\frac{1+D_y}{1-D_y}$
Converter in Fig. 4(c)	1	1	YES	$M=\frac{2}{1-D_y}$
Converter in Fig. 4(d)	1	1	NO	$M=\frac{1+D_y}{1-D_y}$

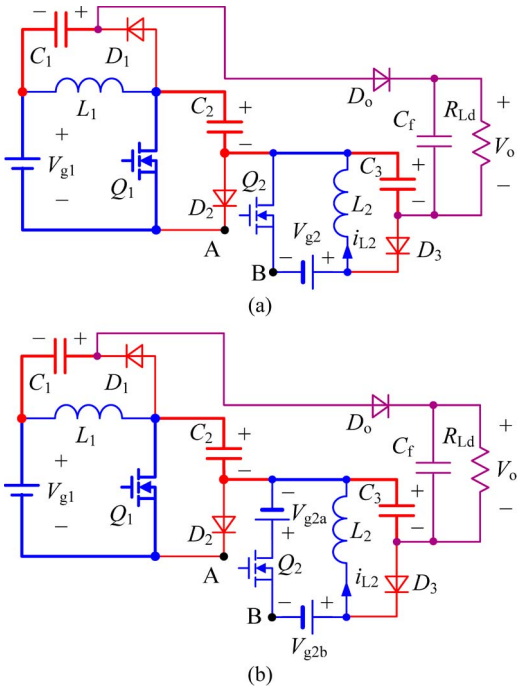

Fig. 9. Extension of a high step-up converter with SIESC-SCs derived from Type-I boost/buck–boost-based converter. (a) Adding one more inductor-energy-storage-cell-based SC. (b) Separating the voltage source V_{g2} into two.

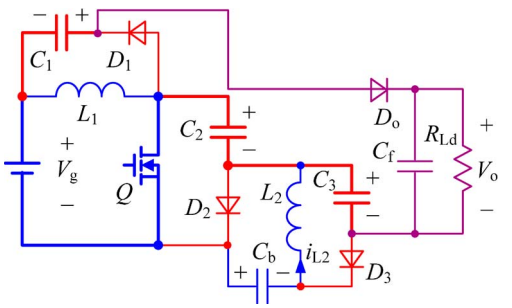

Fig. 10. High step-up converter with double-inductor-energy-storage-cell-based SCs derived from Type-I boost/buck–boost-based converter.

Likewise, based on the converters as shown in Fig. 4(a), (b), and (d), high step-up dc–dc converters with MIESC-SCs are derived as shown in Fig. 12.

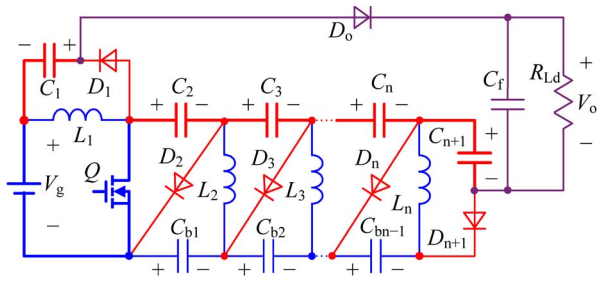

Fig. 11. High step-up converter with MIESC-SCs derived from Type-I boost/buck–boost-based converter.

B. Operating Principle

The operating principles of high step-up converters with MIESC-SCs are similar. Here, the high step-up converter with double inductor energy storage cells derived from Type-I boost/buck–boost-based converter as shown in Fig. 10 is taken as an example to analyze the operating mode. When the inductor current is continuous, there are three operating modes for the converter. Fig. 13 shows the key waveforms of the converter, where v_{gs} is the driving signal of the switch; V_{cb} and V_{c3} are the voltages of C_b and C_3, respectively; and i_{L1} and i_{L2} are the currents of L_1 and L_2. The operating modes are shown in Fig. 14. During $[t_0, t_1]$, switch Q is conducting, and the input voltage source charges L_1, and C_2 charges C_b and L_2. Meanwhile, C_3 and C_2 are in series with the voltage source and C_1 to supply the load through Q. Thus, V_{c3} decreases while V_{Cb} increases. As the voltages of C_b and C_3 are equal before the switch conducts, we have $V_{Cb} > V_{C3}$. During $[t_1, t_2]$, the switch is turned off. Because $V_{Cb} > V_{C3}$, D_3 conducts and D_2 is remaining off. L_1 charges C_1 via D_1, and it charges C_2 and C_3 and discharges C_b. Meanwhile, L_2 charges C_3 via D_3. When V_{C3} increases to V_{Cb}, D_2 conducts, and L_2 charges C_3 and C_b in parallel. Thus, $V_{C3} = V_{Cb}$. At the same time, L_1 charges C_1 through D_1 and charges C_2 through D_2.

At steady state, according to the volt–second relationships of L_1 and L_2, we have

$$V_g D_y T_s = (V_{C2} - V_g)(1 - D_y)T_s$$
$$= V_{C1}(1 - D_y)T_s \quad (8)$$
$$(V_{C2} - V_{Cb})D_y T_s = V_{C3}(1 - D_y)T_s. \quad (9)$$

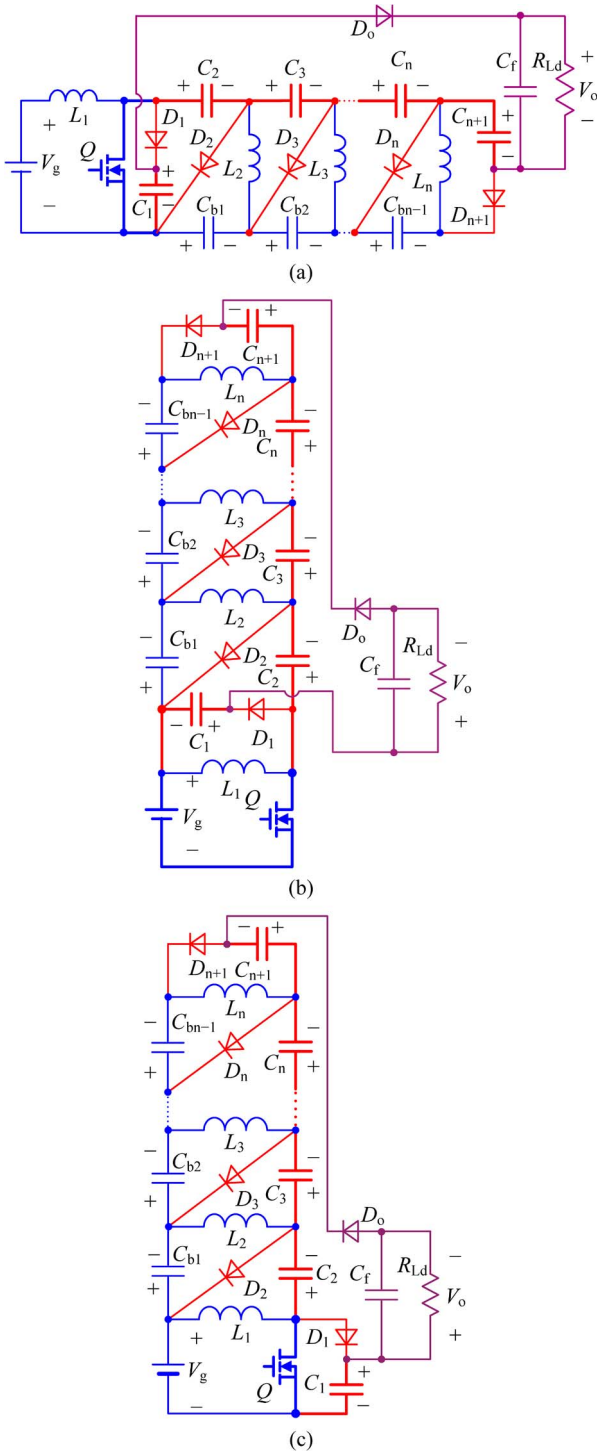

Fig. 12. High step-up converters with MIESC-SCs derived from (a) boost converter, (b) buck–boost converter, and (c) Type-II boost/buck–boost-based converter.

Then,

$$V_{C2} = \frac{V_g}{1 - D_y} \tag{10}$$

$$V_{C1} = V_{C3} = V_{Cb} = \frac{D_y V_g}{1 - D_y}. \tag{11}$$

When Q is on, C_3, C_2, and C_1 are in series with the voltage source to supply the load. Therefore, the voltage gain of the converter can be derived as

$$M = \frac{V_o}{V_g} = \frac{V_{C3} + V_{C2} + V_{C1} + V_g}{V_g} = \frac{2 + D_y}{1 - D_y}. \tag{12}$$

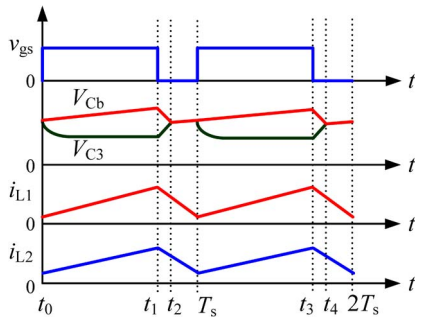

Fig. 13. Key waveforms of high step-up converter with double inductor energy storage cells based SCs derived from Type-I boost/buck–boost-based converter.

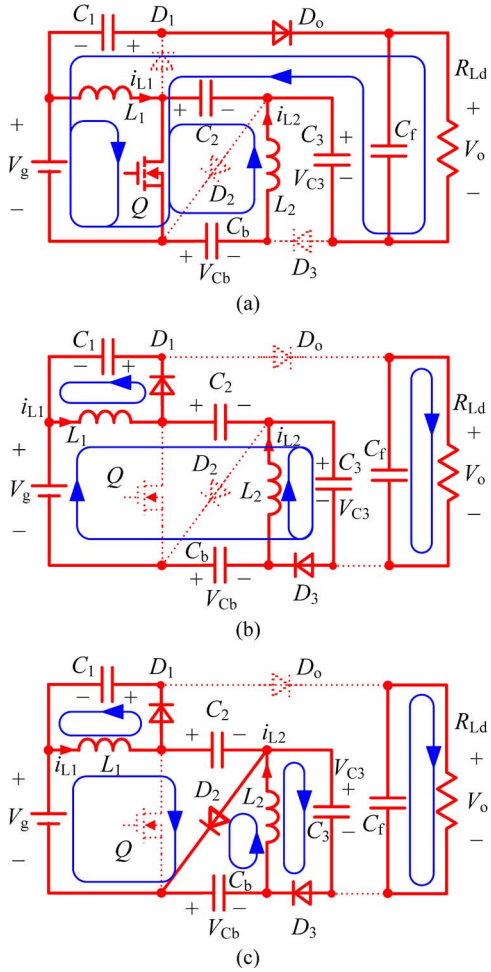

Fig. 14. Operating modes of a high step-up converter with double-inductor-energy-storage-cell-based SCs derived from Type-I boost/buck–boost-based converter. (a) $[t_0, t_1]$. (b) $[t_1, t_2]$. (c) $[t_2, T_s]$.

C. Voltage Gains of High Step-Up Converters With MIESC-SCs

Similar to the derivation of the voltage gain of a high step-up converter with double-inductor-energy-storage-cell-based

TABLE II
VOLTAGE GAINS OF HIGH STEP-UP DC–DC CONVERTERS WITH MIESC-SCS

High step-up dc-dc converter	Voltage gain
High step-up converter with MIESC-SCs derived from boost converter	$M=\frac{2+(n-1)D_y}{1-D_y}$
High step-up converter with MIESC-SCs derived from buck-boost converter	$M=\frac{1+nD_y}{1-D_y}$
High step-up converter with MIESC-SCs derived from Type-I boost/buck-boost-based converter	$M=\frac{2+(n-1)D_y}{1-D_y}$
High step-up converter with MIESC-SCs derived from Type-II boost/buck-boost-based converter	$M=\frac{1+nD_y}{1-D_y}$

SCs derived from Type-I boost/buck–boost-based converter, the voltage gains of the other high step-up converters with MIESC-SCs can be derived, which are listed in Table II, where $M = V_o/V_g$, and n is the number of the inductors.

As illustrated above, the high step-up converters with MIESC-SCs are derived from those with SIESC-SCs by adding more SCs. If the number of the inductors is n, the number of the added SCs is $n-1$. The voltage of each added SC is $V_g D_y/(1-D_y)$; thus, the voltage gains of high step-up converters with MIESC-SCs are increased by $(n-1)D_y/(1-D_y)$.

V. EXPERIMENT VERIFICATION

The high step-up converter with SIESC-SCs derived from Type-I boost/buck–boost-based converter as shown in Fig. 4(c) has a simple circuit configuration and a high voltage gain. Therefore, it is taken as the example to verify the effectiveness of the proposed high step-up dc–dc converters adopting an SC cell. A 100-W output prototype is fabricated in the laboratory with the following specifications: input voltage V_g: 25–45 Vdc; output voltage V_o: 380 Vdc. The switching frequency f_s is 100 kHz.

A. Parameter Design

1) SCs C_2 and C_3: In the above analysis, the SC is regarded as a voltage source. In fact, there exists a small voltage ripple at the switching frequency on the capacitor. When the switch is on, the sum of voltages of C_2 and C_3 and the voltage source is slightly larger than the output voltage. Then, C_2 and C_3 and the voltage source are in series to supply the load. Moreover, the voltage difference is added to the equivalent series resistor (ESR) of the capacitors, which results in large pulsating current. Hence, the voltage ripple should be limited to a small range in case of too large current. As the average current of the branch of filter capacitor C_f is zero, the average current that C_2 and C_3 output to the load when the switch conducts is I_o, where I_o is the load current. Then, the voltage ripples are

$$\begin{cases} \Delta V_{C2} = I_o T_s / C_2 \\ \Delta V_{C3} = I_o T_s / C_3 \end{cases}. \tag{13}$$

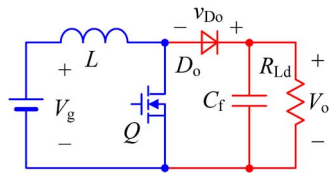

Fig. 15. Basic boost converter.

TABLE III
PARAMETERS OF THE BASIC BOOST CONVERTER AND THE HIGH STEP-UP CONVERTER WITH SIESC-SCS DERIVED FROM TYPE-I BOOST/BUCK–BOOST-BASED CONVERTER

Parameter	Boost converter	High step-up converter with SIESC-SCs derived from Type-I boost/buck-boost-based converter
Input voltage (V)	25 ~ 45	25 ~ 45
Output voltage (V)	380	380
Full load (W)	100	100
Switching frequency (kHz)	100	100

If the ripple voltage is set to 1% of the output voltage, $C_2 = C_3 = 0.693\ \mu$F. Here, 0.82 μF is selected.

2) Boost Inductor L: The boost inductor is designed to limit the maximum current ripple to 20% of the maximum average inductor current. When $P_o = 100$ W and $V_g = 25$ V, the average inductor current is the largest, i.e., $I_{L\_max} = 4$ A. Then, the ripple current is $\Delta i_L = 0.8$ A.

The expression of the ripple current can be given as

$$\Delta i_L = \frac{V_g D_y T_s}{L} = \frac{V_o(1-D_y)D_y T_s}{2L}. \tag{14}$$

Since 25 V $\le V_g \le$ 45 V and $V_o = 380$ V, D_y is always larger than 0.5. As seen in (14), the current ripple decreases with the increase of D_y when $D_y \le 0.5$. Thus, the current ripple reaches the largest value at the maximum voltage of 45 V, where $D_y = 0.763$. The substitution of $D_y = 0.763$, $\Delta i_L = 0.8$ A, $V_o = 380$ V, $T_s = 1/\text{fs} = 10\ \mu$s into (14) leads to $L = 430\ \mu$H.

3) Output Filter Capacitor C_f: Considering the high step-up dc–dc converter is cascaded with a single-phase inverter, the voltage ripple is limited to 1% of the output voltage. Thus, the capacitance is [21]

$$C_f = \frac{P_o}{2\pi f_{line} \Delta V_o V_o} = 220\ (\mu\text{F}) \tag{15}$$

where f_{line} is the line frequency, and here $f_{line} = 50$ Hz. In the practical circuit, a 220 μF/630 V with ESR equaling to 0.3 Ω electrolytic capacitor is adopted.

B. Experiment Results

Fig. 15 shows the basic boost converter. To compare the performance of the boost converter and the high step-up converter with SIESC-SCs derived from Type-I boost/buck–boost-based converter, a prototype of the boost converter with the same specifications is also fabricated in the laboratory. The design progress of inductor L and output capacitor C_f in Fig. 15 is the

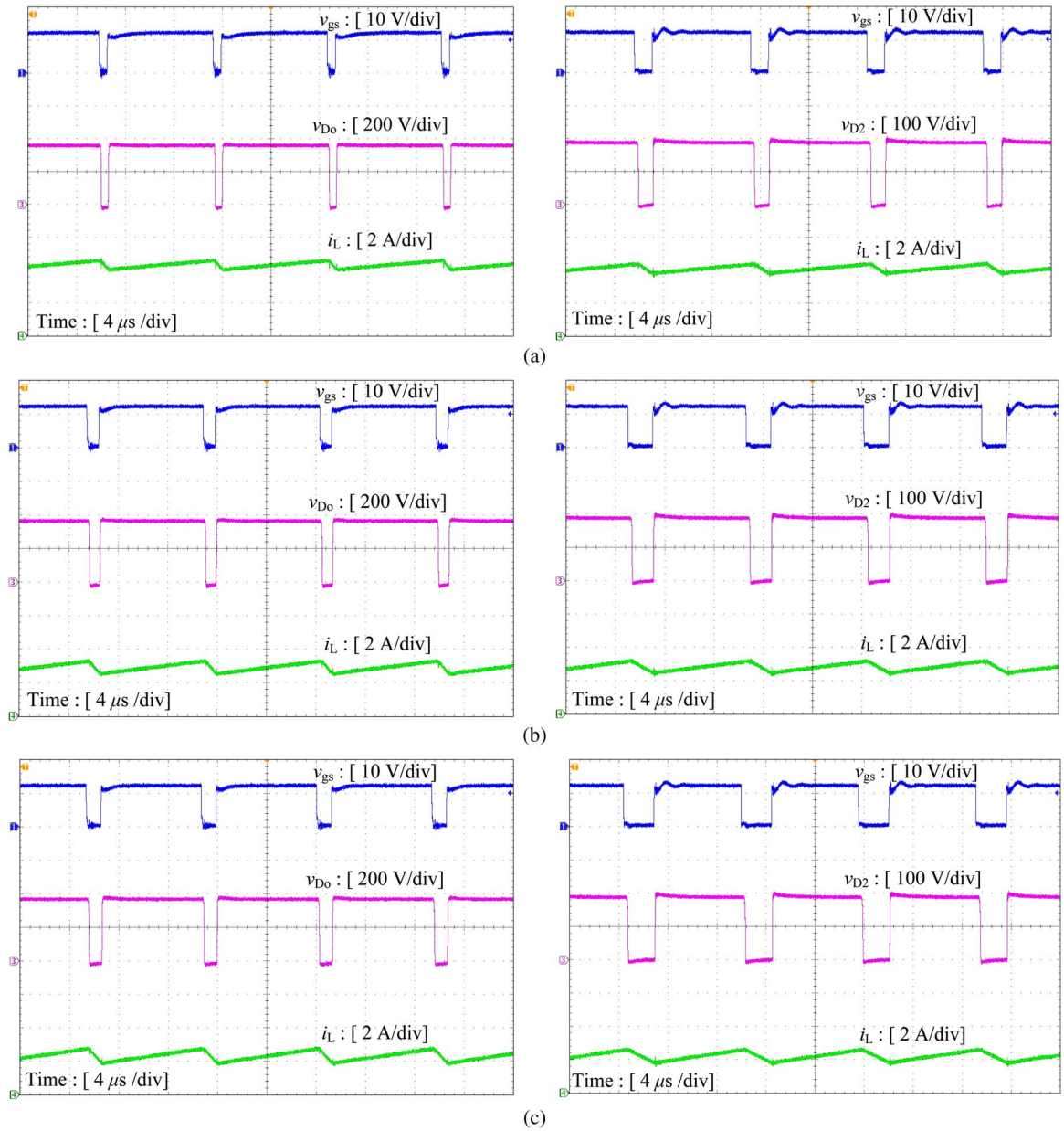

Fig. 16. (Left) Experiment waveforms of boost converter and (right) the high step-up converter with SIESC-SCs derived from Type-I boost/buck–boost-based converter. (a) $V_g = 25$ V. (b) $V_g = 36$ V. (c) $V_g = 45$ V.

same with that of the high step-up converter with SIESC-SCs derived from Type-I boost/buck–boost-based converter. Thus, $L = 500$ μH, and $C_f = 220$ μF. Table III lists the respective parameters.

Fig. 16 gives the experiment waveforms of the boost converter (left) and the high step-up converter with SIESC-SCs derived from Type-I boost/buck–boost-based converter (right) under different input voltages at full load, where v_{gs} is the driving signal of the switch, i_L is the inductor current, v_{Do} is the voltage of the output diode in Fig. 15, and v_{D2} is the voltage of D_2 in Fig. 4(c). When the input voltage is 36 V, the duty cycle of the boost converter is 0.91, whereas the duty cycle of the high step-up converter with SIESC-SCs derived from Type-I boost/buck–boost-based converter is 0.81. Apparently, the high step-up dc–dc converter has a smaller duty cycle than the boost converter. As a result, the inductor current ripple and turn-off current of the switch is lower under the same input and output voltages.

Fig. 17 shows the current waveforms under different input voltages, where v_{gs} is the driving signal, i_Q is the current of the switch, i_{D3} is the current of D_3, and i_{Do} is the current of D_o. In the experiment, a small inductor is added in series with the output diode D_o to suppress the peak current when the switch is turned on. As the inductance is small enough, it has no effect on the operating modes of the proposed converter. Thus, the peak current of D_o shown in Fig. 17 is small. The current spike of the switch shown in Fig. 17 is caused by the reverse recovery of D_2 and D_3. The current of the switch and the duty cycle is larger when the input voltage is low. Therefore, the conduction loss of the switch is larger, and the efficiency is lower.

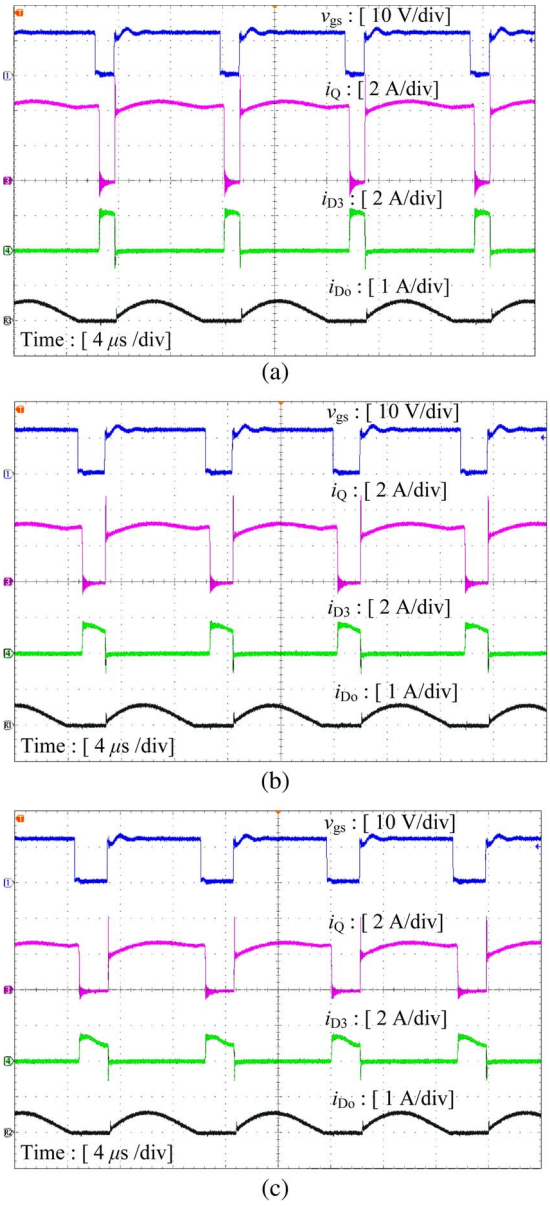

Fig. 17. Experiment waveforms of the high step-up converter with SIESC-SCs derived from Type-I boost/buck–boost-based converter. (a) $V_g = 25$ V. (b) $V_g = 36$ V. (c) $V_g = 45$ V.

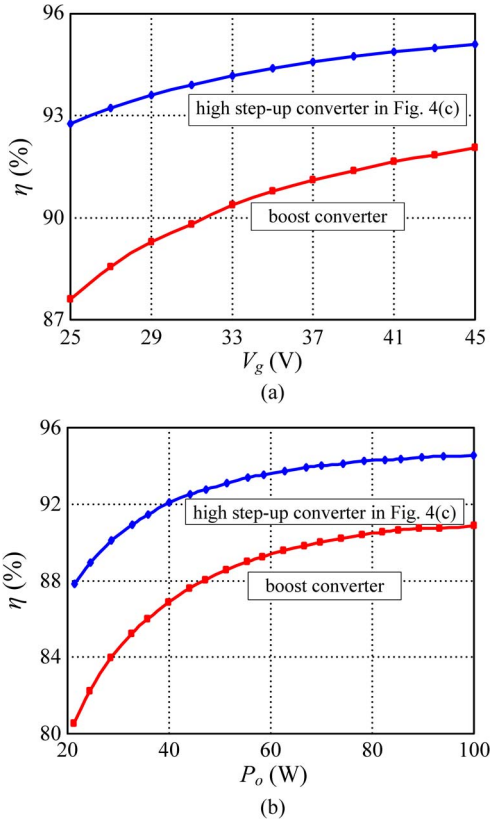

Fig. 18. Measured efficiency curves of the basic boost converter and the high step-up converter with SIESC-SCs derived from Type-I boost/buck–boost-based converter. (a) $P_o = 100$ W. (b) $V_g = 36$ V.

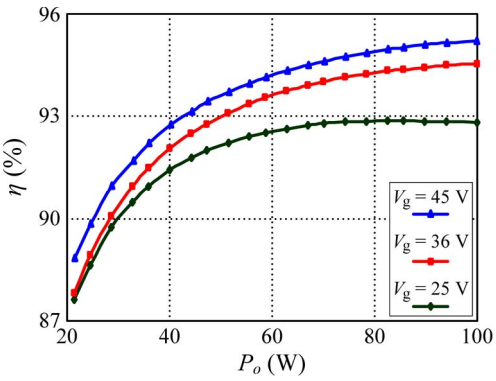

Fig. 19. Measured efficiency curves of the high step-up converter with SIESC-SCs derived from Type-I boost/buck–boost-based converter.

Fig. 18 shows the comparison of the efficiency curves of the boost converter and the high step-up converter under different input voltages and loads. As the duty cycle of the high step-up converter with SIESC-SCs derived from Type-I boost/buck–boost-based converter is smaller, the current ripple and the turn-off current of the switch are lower, leading to less conduction loss and switching loss, which will result in higher conversion efficiency.

Fig. 19 shows measured efficiency curves of the high step-up converter with SIESC-SCs derived from Type-I boost/buck–boost-based converter regarding the load under different input voltages. It can be seen that the efficiency is reduced when the input voltage is low. The phenomenon is explained in the previous paragraph by checking the experimental waveforms in Figs. 16 and 17. As the input voltage decreases, the inductor current i_L remarkably increases, which varies from 2.2 to 4 A. However, the circulating current flowing through the SC i_{Do} is relatively small and independent of the input voltage. When Q is on, the circulating current and the inductor current flow through the switch together. Compared with the inductor current, the circulating current is much smaller. Thus, the conduction loss caused by the circulating current is comparatively small. In fact, despite the small increase in the switch current, a remarkable decrease in the duty cycle is also achieved using the SCs. Therefore, the total conduction loss of the switch is reduced. It is the very reason why the efficiency of the high step-up converter proposed in this paper is higher than that of the basic boost converter.

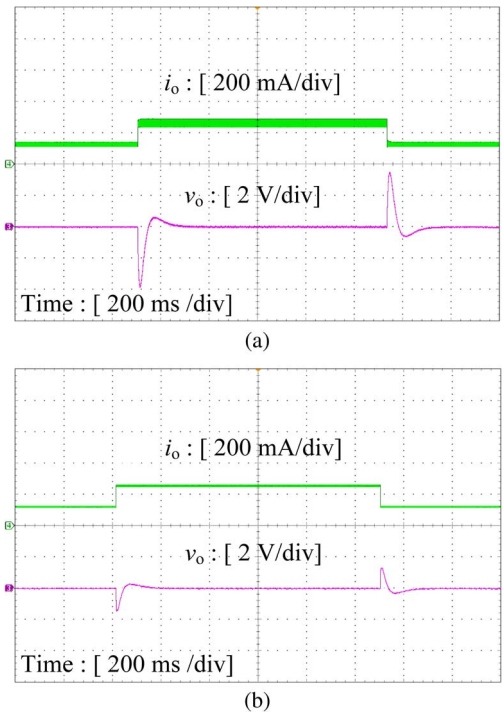

Fig. 20. Load transient experiment waveforms when the load current is step changed between full load and half load. (a) Boost converter. (b) High step-up converter with SIESC-SCs derived from Type-I boost/buck–boost-based converter.

Fig. 20 shows the load transient experiment waveforms of the boost converter and high step-up converter with SIESC-SCs derived from Type-I boost/buck–boost-based converter when the load current is step changed between full load and half load. As seen, both of the overshoot and undershoot of the output voltage of the high step-up converter during load transient are smaller than that of the boost converter. Moreover, the settling time of the output voltage of the high step-up converter during load transient is close to that of the boost converter.

The characteristic of PV and fuel cells is that the output voltage is low and varies in a wide range. To verify that the proposed converters are suitable for the application, the input voltage in the experiment is set at a low voltage with a wide range, i.e., 25–45 V, which is the normal range of PV and fuel cells. The experiment results shown in Figs. 16–18 illustrate that the proposed high step-up converters adopting an SC cell operates with a smaller duty cycle, and the efficiency is higher, compared with the basic boost converter. Fig. 20 shows that the dynamic performance of the high step-up converter adopting an SC cell is better than that of the boost converter.

The efficiency is estimated as shown in Fig. 21, which is close to the experiment results. Table IV gives the loss distribution when $V_g = 36$ V and $P_o = 100$ W, where the power loss of the switch consists of conduction loss and switching loss, the power loss of the diode consists of conduction loss and reverse recovery loss, and the power loss of the inductor consists of core loss and copper loss. According to Table IV, the loss of the switch is dominant, and the total power loss caused by three diodes is the second largest.

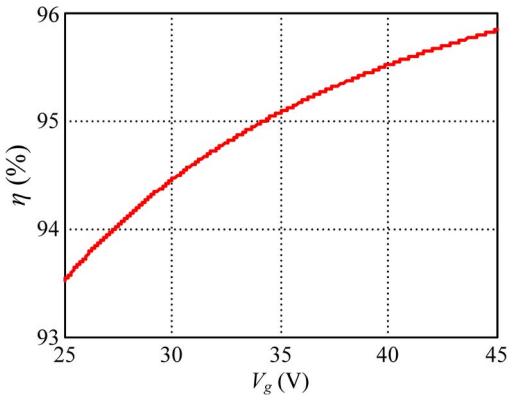

Fig. 21. Estimated efficiency of the high step-up converter with SIESC-SCs derived from Type-I boost/buck–boost-based converter.

TABLE IV
LOSS DISTRIBUTION ($V_G = 36$ V, $P_O = 100$ W)

Device	R_{dson}/ESR (Ω)	V_f (V)	RMS current (A)	Average current (A)	Power loss (W)	Power loss ratio
Q	0.23	–	2.75	–	2.69	52.7 %
D_2	–	1.5	–	0.26	0.52	10.2 %
D_3	–	1.5	–	0.26	0.52	10.2 %
D_o	–	1.5	–	0.26	0.52	10.2 %
L	0.05	–	2.78	–	0.83	16.3 %
C_f	0.3	–	0.065	–	0.02	0.4 %

When a relatively high voltage gain is needed, the converters shown in Figs. 11 and 12 are required at the price of more components. In this situation, incorporating a coupled inductor or transformer has an advantage and definitely increases the voltage gain of the converter with a smaller component count. When the difference of the output voltage and the input voltage is not very large, the voltage gains of the converters in Fig. 4 in this paper, which have simpler structures, are suitable to achieve high efficiency. Thus, the converters proposed in this paper provide various choices for different applications.

VI. CONCLUSION

Based on the respective merits of the SC converter and the switching-mode dc–dc converter, a new method of combination of the SC converter and switching-mode dc–dc converter has been proposed. The combination approach is that when the switch is turned off, the energy stored in the inductor is released to charge the multiple capacitors in parallel whose voltages are controlled by a pulsewidth modulation technique; when the switch is turned on, the capacitors are in series to supply the load. Thus, the voltage gain of the dc–dc converter is increased. The operating mode of a high step-up dc–dc converter adopting an SC cell proposed in this paper was analyzed, and an experiment was conducted. The results indicate that the converters proposed in this paper can steadily operate and that the performance is good.

REFERENCES

[1] J. Leyva-Ramos, J. M. Lopez-Cruz, M. G. Ortiz-Lopez, and L. H. Diaz-Saldierna, "Switching regulator using a high step-up voltage converter for fuel-cell modules," *IET Power Electron.*, vol. 6, no. 8, pp. 1626–1633, Sep. 2013.

[2] G. Velasco-Quesada, F. Guinjoan-Gispert, R. Piqué-López, M. Román-Lumbreras, and A. Conesa-Roca, "Electrical PV array reconfiguration strategy for energy extraction improvement in grid-connected PV systems," *IEEE Trans. Ind. Electron.*, vol. 56, no. 11, pp. 4319–4331, Nov. 2009.

[3] K. Tseng and C. Huang, "High step-up high-efficiency interleaved converter with voltage multiplier module for renewable energy system," *IEEE Trans. Ind. Electron.*, vol. 61, no. 3, pp. 1311–1319, Mar. 2014.

[4] C. Young, M. Chen, T. Chang, C. Ko, and K. Jen, "Cascade Cockcroft–Walton voltage multiplier applied to transformerless high step-up dc–dc converter," *IEEE Trans. Ind. Electron.*, vol. 60, no. 2, pp. 523–537, Feb. 2013.

[5] S. Chen, T. Liang, L. Yang, and J. Chen, "A boost converter with capacitor multiplier and coupled inductor for ac module applications," *IEEE Trans. Ind. Electron.*, vol. 60, no. 4, pp. 1503–1511, Apr. 2013.

[6] M. W. Ellis, M. R. von Spakovsky, and D. J. Nelson, "Fuel cell systems: Efficient, flexible energy conversion for the 21st century," *Proc. IEEE*, vol. 89, no. 12, pp. 1808–1818, Dec. 2001.

[7] W. Li and X. He, "Review of nonisolated high-step-up dc/dc converters in photovoltaic grid-connected applications," *IEEE Trans. Ind. Electron.*, vol. 58, no. 4, pp. 1239–1250, Apr. 2011.

[8] J. Lee, T. Liang, and J. Chen, "Isolated coupled-inductor-integrated dc–dc converter with nondissipative snubber for solar energy applications," *IEEE Trans. Ind. Electron.*, vol. 61, no. 7, pp. 3337–3348, Jul. 2014.

[9] D. Meneses, F. Blaabjerg, O. Garcia, and J. A. Cobos, "Review and comparison of step-up transformerless topologies for photovoltaic AC—Module application," *IEEE Trans. Power Electron.*, vol. 28, no. 6, pp. 2649–2663, Jun. 2013.

[10] M. Prudente, L. L. Pfitscher, G. Emmendoerfer, E. F. Romaneli, and R. Gules, "Voltage multiplier cells applied to non-isolated dc–dc converters," *IEEE Trans. Power Electron.*, vol. 23, no. 2, pp. 871–887, Mar. 2008.

[11] Y. Hsieh, J. Chen, T. Liang, and L. Yang, "Novel high step-up dc–dc converter for distributed generation system," *IEEE Trans. Ind. Electron.*, vol. 60, no. 4, pp. 1473–1482, Apr. 2013.

[12] K. Park, G. Moon, and M. Youn, "Nonisolated high step-up stacked converter based on boost-integrated isolated converter," *IEEE Trans. Power Electron.*, vol. 26, no. 2, pp. 577–587, Feb. 2011.

[13] Q. Zhao and F. C. Lee, "High-efficiency, high step-up dc–dc converters," *IEEE Trans. Power Electron.*, vol. 18, no. 1, pp. 65–73, Jan. 2003.

[14] R. Wai, C. Lin, and C. Chu, "High step-up dc–dc converter for fuel cell generation system," in *Proc. 30th Annu. Conf. IEEE Ind. Electron. Soc.*, 2004, pp. 57–62.

[15] R. Wai and C. Lin, "High-efficiency, high-step-up dc–dc converter for fuel-cell generation system," *IEE Proc.–Elect. Power Appl.*, vol. 152, no. 5, pp. 1371–1378, Sep. 2005.

[16] T. Wu, Y. Lai, J. Hung, and Y. Chen, "Boost converter with coupled inductors and buck–boost type of active clamp," *IEEE Trans. Ind. Electron.*, vol. 55, no. 1, pp. 154–162, Jan. 2008.

[17] T. Wu, Y. Lai, J. Hung, and Y. Chen, "An improved boost converter with coupled inductors and buck–boost type of active clamp," in *Conf. Rec. IEEE IAS Annu. Meeting*, 2005, vol. 1, pp. 639–644.

[18] E. H. Ismail, M. A. Al-Saffar, A. J. Sabzali, and A. A. Fardoun, "A family of single-switch PWM converters with high step-up conversion ratio," *IEEE Trans. Circuits Syst. I, Reg. Papers*, vol. 55, no. 4, pp. 1159–1171, May 2008.

[19] F. Luo and H. Ye, "Positive output super-lift converters," *IEEE Trans. Power Electron.*, vol. 18, no. 1, pp. 105–113, Jan. 2003.

[20] F. Luo, "Investigation on split-capacitors applied in positive output super-lift Luo-Converters," in *Proc. Chinese Control Decision Conf.*, 2011, pp. 2792–2797.

[21] L. Gu, X. Ruan, M. Xu, and K. Yao, "Means of eliminating electrolytic capacitor in ac/dc power supplies for LED lightings," *IEEE Trans. Power Electron.*, vol. 24, no. 5, pp. 1399–1408, May 2009.

Gang Wu (S'12) was born in Jiangsu, China, in 1989. He received the B.S. degree in electrical engineering and automation from Nanjing University of Aeronautics and Astronautics, Nanjing, China, in 2011, where he is currently working toward the Ph.D. degree in electrical engineering.

His current research interests include high step-up dc–dc converters and renewable energy generation systems.

Xinbo Ruan (M'97–SM'02) received the B.S. and Ph.D. degrees in electrical engineering from Nanjing University of Aeronautics and Astronautics (NUAA), Nanjing, China, in 1991 and 1996, respectively.

In 1996, he joined the College of Automation Engineering, NUAA, where he became a Professor in 2002. Since March 2008, he has been with the College of Electrical and Electronic Engineering, Huazhong University of Science and Technology, Nanjing. He is the author or coauthor of five books and more than 180 technical papers published in journals and conference proceedings. His main research interests include soft-switching power electronics converters, power electronics system integration, and renewable energy generation systems.

Dr. Ruan was the Vice President of the China Power Supply Society from 2005 to 2013. He has been an Associate Editor for the IEEE TRANSACTIONS ON INDUSTRIAL ELECTRONICS and the IEEE JOURNAL OF EMERGING AND SELECTED TOPICS ON POWER ELECTRONICS since 2011 and 2013, respectively.

Zhihong Ye (M'00) was born in Zhejiang, China, in 1969. He received the B.S. and M.S. degrees in electrical engineering from Tsinghua University, Beijing, China, in 1992 and 1994, respectively, and the Ph.D. degree from the Bradley Department of Electrical and Computing Engineering, Virginia Polytechnic Institute and State University, Blacksburg, VA, USA, in 2000.

From 2000 to 2005, he was an Electrical Engineer with the General Electric Global Research Center, Niskayuna, NY, USA. From 2005 to 2006, he was a Commodity Quality Manager with Dell. Since 2006, he has been the Director of Research and Development with Lite-On Technology Corporation, Nanjing, China. He holds 17 U.S. patents and has published more than 30 technical papers in journals and international conference proceedings. His research interests include high-density high-efficiency power supplies for computing, communication and consumer electronics applications, digital control, power converter topologies and controls, and soft-switching techniques.